

RESEARCH

Open Access



Systematic multiomics analysis and in vitro experiments suggest that ITGA5 could serve as a promising therapeutic target for ccRCC

Xiangxian Che^{1,3†}, Xi Tian^{1,2,3†}, Zhenda Wang^{1,2,3†}, Shuxuan Zhu^{1,2,3}, Shiqi Ye^{1,2,3}, Yue Wang^{1,2,3}, Yihan Chen³, Yiyun Huang³, Aihetaimujiang Anwaier^{1,2,3}, Peifeng Yao⁴, Yijia Chen³, Keting Wu³, Yifei Liu³, Wenhao Xu^{1,2,3*}, Hailiang Zhang^{1,2,3*} and Dingwei Ye^{1,2,3*}

Abstract

Background Integrin alpha 5 (ITGA5) was previously confirmed to be related to prognosis in several cancer types; however, its function in clear cell renal cell carcinoma (ccRCC) and how this molecule regulates tumor progression and the tumor microenvironment (TME) remain to be elucidated.

Methods We investigated the prognostic implications of ITGA5 with a machine learning model and evaluated biological behaviors of different levels of ITGA5 expression in vitro. Bioinformatic analysis was performed to explain the comprehensive effect of ITGA5 on the TME and drug sensitivity.

Results We constructed a machine learning model to elaborate the prognostic implication of ITGA5. As tumorigenesis of ccRCC was tightly relevant with several mutant genes, we investigated the correlation between ITGA5 expression and frequent mutations and found ITGA5 upregulation in VHL mutant ccRCC ($P=0.016$). Through overexpressing, silencing, and blocking ITGA5, we verified the role of ITGA5 in promoting ccRCC adverse biological activities; and the potential functions of ITGA5 in ccRCC were bioinformatically demonstrated, summarizing as cell proliferation, migration, and angiogenesis. The localization of ITGA5 primarily in endothelia and macrophages further verified its magnitude in angiogenesis and aroused our excavation in ITGA5 regulation of immune infiltration landscape. Generally, ITGA5-high ccRCC presented an immunosuppressive TME by inducing a lower level of CD8 + T cell infiltration. For the last part we predicted drug sensitivity relevant to ITGA5 and concluded that a joint medication of ITGA5 inhibitors and VEGFR-target drugs (including sunitinib, axitinib, pazopanib, and motesanib) might be a promising therapeutic strategy.

Conclusion Our findings clarified the adverse outcome induced by high expression of ITGA5 in ccRCC patients. In vitro experiments and bioinformatical analysis identified ITGA5 function as predominantly cell proliferation, migration, angiogenesis, and macrophage recruitment. Further, we predicted immune infiltration and medication sensitivity

[†]Xiangxian Che, Xi Tian and Zhenda Wang have contributed equally.

*Correspondence:

Wenhao Xu
xwhao0407@163.com
Hailiang Zhang
zhanghl918@163.com
Dingwei Ye
dwyelie@163.com

Full list of author information is available at the end of the article



© The Author(s) 2024. **Open Access** This article is licensed under a Creative Commons Attribution-NonCommercial-NoDerivatives 4.0 International License, which permits any non-commercial use, sharing, distribution and reproduction in any medium or format, as long as you give appropriate credit to the original author(s) and the source, provide a link to the Creative Commons licence, and indicate if you modified the licensed material. You do not have permission under this licence to share adapted material derived from this article or parts of it. The images or other third party material in this article are included in the article's Creative Commons licence, unless indicated otherwise in a credit line to the material. If material is not included in the article's Creative Commons licence and your intended use is not permitted by statutory regulation or exceeds the permitted use, you will need to obtain permission directly from the copyright holder. To view a copy of this licence, visit <http://creativecommons.org/licenses/by-nc-nd/4.0/>.

regulation by ITGA5 and proposed a joint use of ITGA5 inhibitors and anti-angiogenetic drugs as a potential potent therapeutic strategy.

Keywords Clear cell renal cell carcinoma, ITGA5, Biomarker, Machine learning, Tumor microenvironment

Introduction

Renal cell carcinoma (RCC) stands as a prominent malignancy within the urinary system. As evidenced by the US 2024 cancer statistics, renal cell carcinoma accounts for approximately 4% of all diagnosed cancer cases, ranking as the sixth most common cancer in males and the ninth in females [1]. Data from China's 2016 cancer registry indicate a crude incidence of kidney cancer of 5.48 per 100,000 individuals, translating to an estimated 75,800 new cases annually [2]. ccRCC comprising roughly 75% of RCC cases, represents the most prevalent and lethal histological subtype. Notably, ccRCC is featured by prominent immune and vascular infiltration [3, 4]. In the realm of ccRCC treatment, tyrosine kinase inhibitors (TKIs) currently receive primary recommendations [5]. Additionally, immune checkpoint blockade (ICB) therapy, has emerged as a revolutionary therapy demonstrating unprecedented progress in oncology, and is now frequently employed in conjunction with targeted therapies [6]. Nonetheless, in the context of ccRCC, established genomic correlates of ICB response in solid tumors, such as tumor mutation burden (TMB) and PD-L1 status, have not demonstrated predictive value in ccRCC [7, 8], highlighting the imperative need to identify robust biomarkers that can forecast ICB responsiveness and refine patient selection for this treatment modality.

Integrins comprise a family of at least 24 heterodimeric transmembrane receptors that mediate cell adhesion to a diverse array of extracellular matrix (ECM) components. Acting as crucial sensors of the microenvironment, these receptors exert regulatory control over various cellular activities including survival, proliferation, migration and invasion [9]. A particular process known as integrin-mediated death, where unbound integrins trigger apoptosis via caspase 8 activation, underscores the critical role of integrins in cellular fate [10]. Integrins expressed by host cells also play a significant role in supporting tumor progression, such as angiogenesis [11], the most significant hallmark feature of renal cell carcinoma.

Among integrins, ITGA5 mainly functions as a receptor of fibronectin in form of a heterodimer combined with integrin beta 1 [12]. Recognized as an essential bridge molecule of FAK-ITGA5-Akt axis, ITGA5 is highly expressed in a panel of tumors and results in poor prognosis, through inducing bone metastasis of breast cancer [13], inducing temozolomide and bevacizumab resistance in gliomas [14], and promoting anti-androgen

resistance in prostate cancer [15]. Additionally, ITGA5 has been implicated in regulating the tumor microenvironment (TME), influencing not only immune cells such as macrophages, T-helper cells, and natural killer (NK) cells but also endothelial cells and fibroblasts [16–19]. Emerging evidence suggests that ITGA5 expression may serve as a predictor of immune checkpoint blockade (ICB) therapy efficacy [19, 20]. Despite these findings, the role of ITGA5 in the modulation of ccRCC and its associated TME remains to be elucidated.

Our study presents a higher expression of ITGA5 detected in the genomic analysis of 232 tumor and adjacent normal tissue pairs from Fudan University Shanghai Cancer Center (FUSCC) and 535 ccRCC patients from the Cancer Genome Atlas (TCGA). This study aims to elucidate the prognostic significance of ITGA5 and explore its potential role in regulating ccRCC aggressiveness. Bioinformatic approaches are utilized to predict ITGA5 functions and assess immune cell infiltration within the ccRCC TME. Our findings intend to establish ITGA5 as a promising novel therapeutic target for ccRCC.

Materials and methods

Data acquisition and normalization

This research enrolled ccRCC samples from FUSCC (n=232) [21], TCGA (n=535) cohort, and two Gene Expression Omnibus (GEO) datasets [GSE53000 (n=53) and GSE53757 (n=72)]. Gene expression and associated clinical data were extracted and differentially expressed genes were identified using the limma package [22]. Genes with a log2 fold change (FC) > 1 and an adjusted P value < 0.05 were classified as upregulated. Somatic mutation data of TCGA-KIRC patients were also obtained to evaluate potential correlations between gene expression and somatic mutations. Additionally, single-cell RNA sequencing data from GEO datasets GSE139555 and GSE171306 were analyzed to determine ITGA5 distribution in TME cell populations. Available clinicopathological features were listed in Table 1.

Depmap gene dependency

The Cancer Dependency Map (<https://depmap.org/portal/>) was a publicly accessible online resource that integrates data from large-scale multiomics screening projects, including the Cancer Cell Line Encyclopedia (CCLE) [23] and the Achilles Project based on

Table 1 Clinicopathological features

	FUSCC cohort (n = 232)	TCGA cohort (n = 535)
Age (y), median (IQR)	–	61 (52, 70)
Gender (n, %)		
Male	157 (67.7%)	349 (65.2%)
Female	75 (32.3%)	186 (34.8%)
Stage (n, %)		
I	157 (67.7%)	269 (50.3%)
II	30 (12.9%)	58 (10.8%)
III	25 (10.8%)	123 (23.0%)
IV	20 (8.6%)	82 (15.3%)
T (n, %)		
T1	162 (69.8%)	275 (51.4%)
T2	36 (15.5%)	70 (13.1%)
T3	31 (13.4%)	179 (33.5%)
T4	3 (1.3%)	11(2.0%)

IQR Interquartile range

genome-scale CRISPR-Cas9 knockout screens [24]. Simply, the gene effect scores evaluated the effect size of knocking out or knocking down a gene while normalizing expression against the distribution of pan-essential and nonessential genes. Negative scores indicate that knocking out or down a gene hinders cell line growth, while positive scores suggest enhanced growth following the experimental manipulation.

Prognostic implication validation and machine learning model construction

Kaplan–Meier curves were generated to assess the prognostic significance of ITGA5 expression in ccRCC patients. The optimal cut-off value for ITGA5 expression, demarcating high and low expression groups, was determined using the R package survminer. A cohort of 535 TCGA-KIRC patients was utilized to construct prognostic models. Lasso regression was employed for feature selection to identify hub genes from differentially expressed genes in the ITGA5 high/low expression groups. With these genes, eXtreme Gradient Boosting (XGBoost), a well-established machine learning classification algorithm, was implemented to model the data [25]. Through parameter tuning, the objective function was continuously optimized to achieve optimal performance. The TCGA-KIRC cohort was randomly partitioned into training and testing sets at a 4:1 ratio. The receiver operating characteristic (ROC) curve was generated using the “survival ROC” R package to calculate the mean area under the curve (AUC).

Mutation landscape regulated by ITGA5

Mutation annotation format (MAF) files were retrieved from TCGA database (<https://portal.gdc.cancer.gov/repository>). Correlation analysis was performed between frequently mutant genes in ccRCC and ITGA5 expression level in TCGA cohort and FUSCC cohort. We visualized mutation data using the MAFtools package (<http://biocoductor.org/packages/maftools/>).

Quantitative real-time PCR (qRT-PCR)

qRT-PCR assays were performed as previously described [26]. GAPDH was employed as an internal control. Relative mRNA expression was determined using the 2– $\Delta\Delta$ ct method. Primer sequences used for amplification were provided in supplementary table.

Western blotting

Cells were harvested by scraping into an SDS sample buffer containing a inhibitor cocktail. Western blotting was performed according to previous description [27]. Antibodies were listed in supplementary table.

Cell culture and transfection

Cells were cultured in RPMI-1640 media supplemented with 10% fetal bovine serum (FBS), 100 U/ml penicillin and streptomycin at 37 °C in a humidified atmosphere of 5% CO₂. Cells were seeded in six-well plates and transfected respectively with small interfering RNA (siRNA) and with an ITGA5 overexpression plasmid using Lipofectamine 2000 reagent. The siRNA sequences were provided in supplementary table. Cells were harvested and used for experiments 48 h post-transfection.

Cell counting kit-8 (CCK-8) assay

Transfected cells were seeded onto 96-well plates at a density of 2000 cells per well. Cells were incubated with 100 μ L fresh medium with 10 μ L CCK8 for 2 h at 37 °C. Absorbance readings at 450 nm of each well ware measured every 24 h for 5 days. Three biological replicates were conducted for each sample.

Wound healing assay

Wound healing assays were performed to assess the migratory ability of 786-O and 769P cells. After 48 h of transfection, the cell monolayer was gently scratched using a 200 μ L Eppendorf tip to create a wound at 90% confluency. Detached cells removed and serum-free medium incubated, the 6-well plate was observed under a light microscope after 12 h.

Transwell assay

A total of 20,000 cells were seeded on the top of a polycarbonate Transwell filter with 200 μ L culture medium

without fetal bovine serum. The lower compartment was filled with 800 µl complete culture medium. A layer of Matrigel was spread on the upper surface of the Transwell filter. After incubation for 24 h, the cells were fixed with 4% paraformaldehyde solution and stained with crystal violet.

Peptidomimetics

The ITGA5 inhibitor was designed by Praneeth R. Kuntinty et al. to mimic domain 9 and 10 of fibronectin that interacts with ITGA5 [28]. Prior research has validated the interaction between this peptide and ITGA5. The peptides were stored at -80°C and dissolved in 1640 culture medium to make up of different concentrations of solutions.

Exploration of potential function of ITGA5

Based on differentially expressed genes between different ITGA5 expression patterns, Gene Ontology (GO) annotation, Kyoto Encyclopedia of Genes and Genomes (KEGG) pathway enrichment analyses, and Gene set enrichment analysis (GSEA) were conducted with the “clusterProfiler” package to compare pathway enrichment between ITGA5 high and low expressed cells. Gene Ontology molecular function gene sets were obtained from <http://www.gsea-msigdb.org/gsea/msigdb>. Predefined gene sets from the Molecular Signatures Database (v.7.4) in GSEA software (v4.1.0) were used for analysis [29]. All basic and advanced fields were set to default. To further describe the function landscape of ITGA5, protein–protein interaction (PPI) network was constructed by the GeneMANIA website (<http://genemania.org>) and Cytoscape. GeneMANIA identified functionally similar genes by protein–protein, protein–DNA interactions, pathways, physiological and biochemical reactions, co-expression, co-localization [30]. Besides, the Search Tool for the Retrieval of Interacting Genes (STRING; <http://string-db.org>) (version 11.0) [31] was searched to demonstrate the interaction between proteins. Differentially expressed genes in ITGA5 low/high group were uploaded to STRING and the retrieved interaction data of these proteins were analyzed in Cytoscape (version 3.9.1) using Density of Maximum Neighborhood Component (DMNC) algorithm in CytoHubba plugin. The top 20 interacting proteins were identified as hub genes and then used to construct the core PPI network. Proteins with minimal interactions were excluded to enhance network clarity and focus on the most relevant connections.

Tumor microenvironment evaluation

Stromal scores were calculated by applying the ESTIMATE algorithm to the downloaded database [32]. Immune infiltration was calculated by CIBERSORT [33]

and Tumor Immune Estimation Resource (TIMER2.0, <http://timer.cistrome.org>). Count values of detected RNA levels were first transformed to transcripts per million (TPM) value format. The transformed gene expression matrix, encompassing data from 535 samples, was uploaded and run with the following indexes selected: relative and absolute modes together, LM22 signature gene file, 1000 permutations, and quantile normalization disabled.

Drug response prediction

The R package pRRophetic was employed to predict potential drug responses for samples categorized into ITGA5 high and low expression groups [34]. The analysis leveraged pharmacogenomic data obtained from the Genomics of Drug Sensitivity in Cancer (GDSC) database [35]. Specifically, the TCGA-KIRC cohort data was used to predict drug sensitivity based on ITGA5 expression. The half maximal inhibitory concentration (IC50) value was calculated by pRRophetic package to reflect the drug response. Besides, tumor immune dysfunction and exclusion (TIDE) analysis were performed. TIDE is an analytical tool that predicts immunotherapy response by considering T cell dysfunction and exclusion from the tumor microenvironment [36]. Processed data were uploaded to the TIDE web portal (<http://tide.dfci.harvard.edu/>) to output predictive ICB response. Patients with lower TIDE score are predicted to be more responsive to immunotherapy.

Statistical analysis

All numerical data were presented as the mean \pm SD. Statistical analyses and graph visualizations were conducted using R studio (version 4.1.3) and GraphPad Prism (version 10.1.0). Pearson test or t test was applied to compare the differences between the two groups. For survival analysis, the Kaplan–Meier method was employed, followed by the log-rank test to assess the significance of differences in survival between groups. A two-sided P value less than 0.05 was considered statistically significant, with asterisks (*) indicating significance levels: * $P < 0.05$; ** $P < 0.01$; *** $P < 0.001$; **** $P < 0.0001$.

Results

Expression of ITGA5 is upregulated in ccRCC

Analysis of proteogenomic sequencing data of 232 paired ccRCC tumor and adjacent non-tumor tissues from FUSCC revealed multiple upregulated pathways related to pathogenesis and progress of ccRCC. Notably, the PI3K–Akt pathway was significantly upregulated in tumor tissues (Fig. 1A). Further investigation identified activation of several genes within this pathway, including ITGA5, GYS2, and TLR2 (Fig. 1B, C).

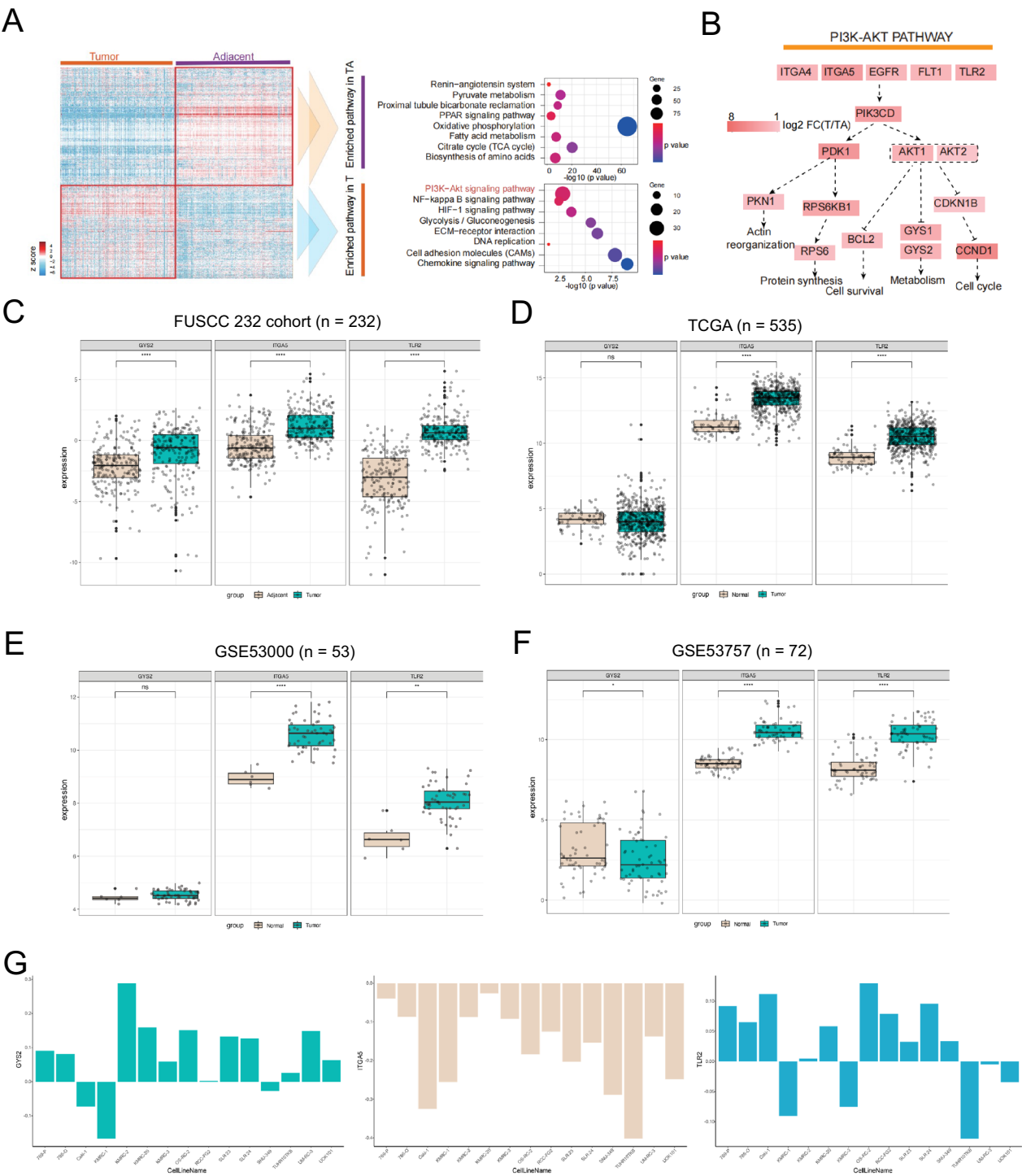


Fig. 1 Expression of ITGA5 is upregulated in ccRCC. **A** Differently expressed proteins and enriched pathways in ccRCC tumor and tumor adjacent regions in FUSCC cohort. **B** Signaling transduction of PI3K-AKT pathway. **C–F** ITGA5, GYS2, and TLR2 expression in FUSCC cohort, TCGA cohort, GSE53000, and GSE53757. **G** Crispr gene effect of ITGA5, GYS2, and TLR2

To identify the potential risk genes associated with tumor progression in ccRCC, we evaluated their expression levels in other cohorts. We observed consistent upregulation of ITGA5 and TLR2, while GYS2 expression displayed no statistical difference in TCGA cohort (Fig. 1D). Analysis of additional datasets

from GEO (GSE53000 and GSE53757) confirmed the consistent upregulation of ITGA5 and TLR2 across different conditions, whereas GYS2 expression remained variable (Fig. 1E, F).

To functionally validate the role of these genes in ccRCC progression, we compared the effects of CRISPR-mediated gene knockouts on ccRCC cell lines from CCLE (Fig. 1G). These experiments identified ITGA5 as the most critical regulator of ccRCC tumor progression. Based on these findings, we selected ITGA5 for further investigation in this study.

Elevated ITGA5 expression signals poor outcome: developing an ITGA5-related prognostic prediction model

To detect clinical relevance of ITGA5, ITGA5 expression levels were evaluated in relation to patient prognosis and Kaplan–Meier analysis revealed a positive correlation between elevated ITGA5 expression and poor outcomes, including overall survival (OS) and disease-free survival (DFS) (Fig. 2A, B). This finding underscores the potential role of ITGA5 as a key biomarker in clinical prognosis.

We constructed a machine learning model to further explore clinical implication value of ITGA5. Among 1988 differentially expressed genes between ITGA5 high and low group, hub genes were first selected by lasso regression analysis (Fig. 2C, D). These hub genes

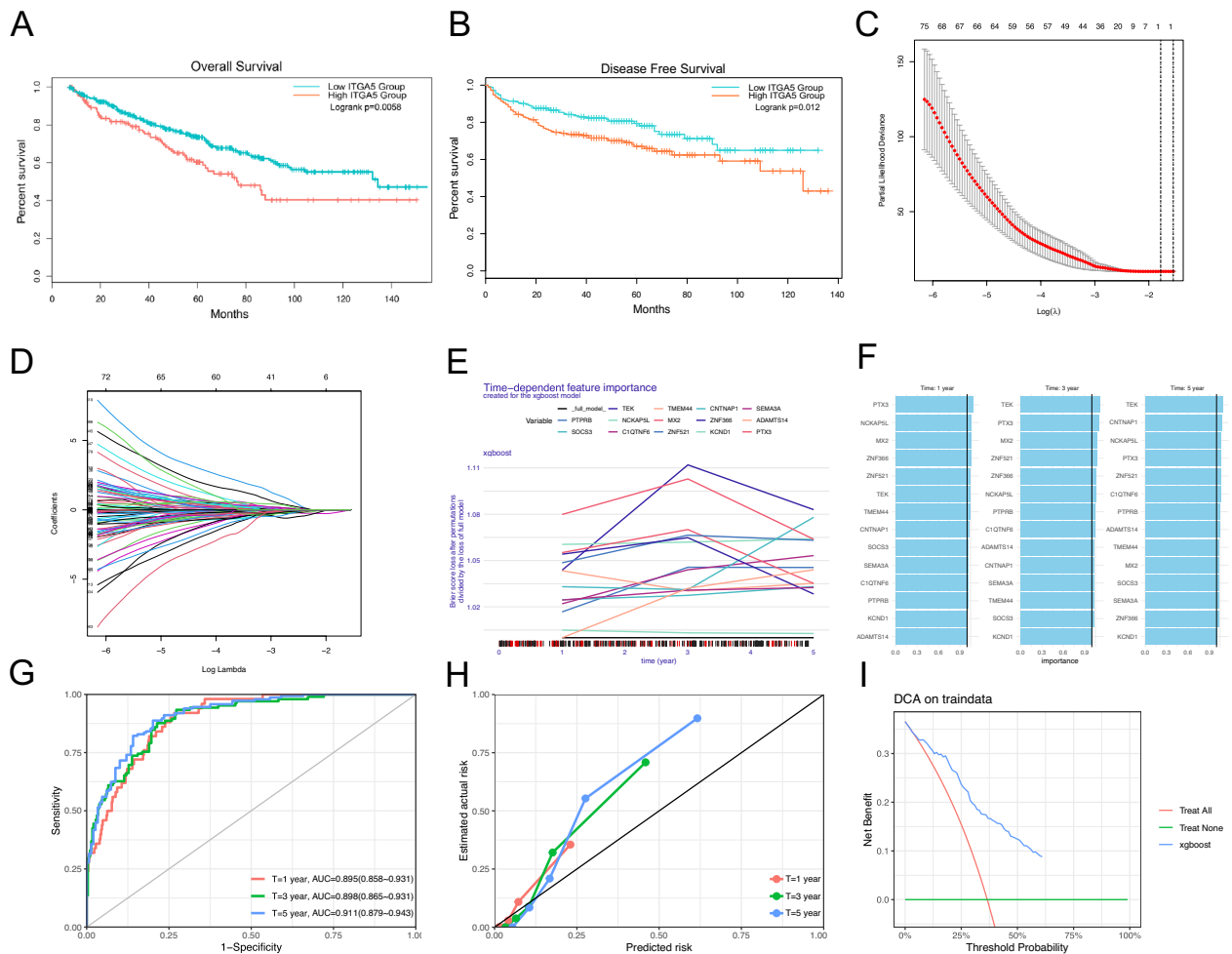


Fig. 2 Elevated ITGA5 expression signals poor outcome: Developing an ITGA5-related Prognostic Prediction Model. **A, B** Kaplan–Meier curves for OS and DFS of patients with different ITGA5 expression. **C, D** Coefficient profiles of 1988 ITGA5-related differentially expressed genes and identification of the best parameter (lambda) according to the least absolute shrinkage and selector operation (LASSO). **E** Time-dependent importance of feature genes. **F** Top important genes in predicting 1-, 3-, 5-year OS. **G** The time-dependent ROC curves of the XGBoost model for predicting the 1-, 3-, and 5-year OS. **H** Calibration plot for the XGBoost-predicted OS and actual OS of ccRCC patients at 1-, 3- and 5-year. **I** DCA of the model for predicting the 1-, 3-, and 5-year OS

were subsequently employed to construct a prognostic model for the TCGA-KIRC cohort via XGBoost, a popular machine learning algorithm. The cohort was divided into a training set and a testing set at a ratio of 4:1. Time-dependent feature importance of these genes was calculated (Fig. 2E), and we focused on the importance of the top genes in a 1-, 3-, 5-year-period (Fig. 2F). The AUCs of ROC curves for 1-, 3-, and 5-year OS were 0.895, 0.898, and 0.911, respectively, highlighting the impressive predictive power of the model (Fig. 2G). Calibration plots corroborated the excellent agreement between predicted and actual OS for ccRCC patients at these time points (Fig. 2H). Besides, DCA substantiated the favorable net benefit conferred by the model (Fig. 2I). These results indicated that the XGBoost model had a robust power to predict the prognosis of ccRCC patients and had potential clinical utility in personalized clinical management.

ITGA5 correlates to typical mutations in ccRCC

ccRCC could be characterized by somatic mutation of several typical genes, most frequently von Hippel-Lindau (VHL). VHL mutations are well-established contributors to ccRCC tumorigenesis and progression [37, 38]. SETD2, PBRM1 and BAP1 are also common mutant genes in ccRCC by engendering genomic instability [37]. Therefore, we investigated ITGA5 expression levels in relation to gene mutation phenotypes compared to the wild-type tumors. Notably, ITGA5 is upregulated in VHL-mutant ccRCC in TCGA cohort (Fig. 3A), implying a potential mechanism of VHL-mutant ccRCC progression. Despite the absence of statistical difference in FUSCC 232 cohort, a similar upward trend was observed (Fig. 3B). Other genes of high mutant frequency in ccRCC did not appear to correlate with ITGA5 expression, both in TCGA cohort and in FUSCC cohort (Figure S1). This could be attributed to the lower mutation rate of these genes, but a trend was still discernible. For instance, a trend of downregulation of ITGA5 was observed in the BAP1 and MTOR mutant groups (Figure S1A, S1B). These findings collectively suggest a potential role for ITGA5 in specific subtypes of ccRCC.

Further, we investigated the mutation landscape within the ITGA5 high and low expression groups. While the three most frequently mutated genes in ccRCC (VHL, PBRM1, and TTN) remained at the forefront, the specific mutated genes differed between the groups (Fig. 3C, D). Notably, the mutation sites within VHL also exhibited variations between the high and low ITGA5 expression groups (Fig. 3E, F). To gain a broader perspective, analysis was extended to visualize these mutation landscape differences across chromosomes (Fig. 3G, H). These results suggested an altered mutation landscape in ITGA5 high/low group; however, the co-regulatory

relationship between ITGA5 and these mutations remain to be elucidated. Further investigation is warranted to define the precise mechanisms by which ITGA5 interacts with specific VHL mutation types and the broader mutation landscape in ccRCC.

ITGA5 promotes malignancy and progression of ccRCC

To investigate the effect of ITGA5 on ccRCC, we first evaluated its expression levels in RCC cell lines available in our laboratory, including three generally-recognized ccRCC cell lines, 786-O, 769P and CAKI-1. We observed significant variation in ITGA5 mRNA expression, with 786-O exhibiting the highest level and 769P as the lowest (Fig. 4A). Based on this finding, we selected 786-O for ITGA5 knockdown and 769P for ITGA5 overexpression experiments.

As confirmed by western blotting assay, we silenced and overexpressed ITGA5 in 786-O and 769P cells, through transducing siRNA and overexpression plasmid of ITGA5 respectively (Fig. 4B). Notably, ITGA5 knockdown also resulted in changes in phosphorylation level of AKT, suggesting potential modulation of the PI3K-Akt pathway (Fig. 4B).

Subsequent functional assays were conducted to investigate how ITGA5 regulates tumor cells, revealing a critical role for ITGA5 in ccRCC progression. Silencing ITGA5 in 786-O cells significantly inhibited cell proliferation as measured by CCK-8 assay (Fig. 4C). Conversely, ITGA5 overexpression in 769P cells promoted enhanced proliferation (Fig. 4D). Transwell assays demonstrated that ITGA5 overexpression increased cell invasion capacity, while knockdown had the opposite effect (Fig. 4E, F). Similarly, wound healing assays confirmed that ITGA5 silencing impaired cell migration, whereas overexpression enhanced it (Fig. 4G, H). Collectively, these findings identified ITGA5 as a key promoter of malignancy and progression in ccRCC.

Given the pro-tumorigenic effects of ITGA5, we next investigated the potential for therapeutic intervention using a previously established ITGA5 inhibitor (Arg-Tyr-Tyr-Arg-Ile-Thr-Tyr) [28]. We treated 786O cells, chosen for their high ITGA5 expression, with varying concentrations of the inhibitor (NC, 5 μ M, 10 μ M, 20 μ M, and 50 μ M). Similar to the functional assays with ITGA5 modulation, we employed wound healing, transwell, and CCK-8 assays to assess the inhibitor's efficacy. As expected, treatment with the ITGA5 inhibitor resulted in dose-dependent suppression of cell migration (Fig. 4I), invasion (Fig. 4J), and proliferation (Fig. 4K). These findings further substantiate the critical role of ITGA5 in ccRCC progression and suggest the potential therapeutic value of ITGA5 inhibition.

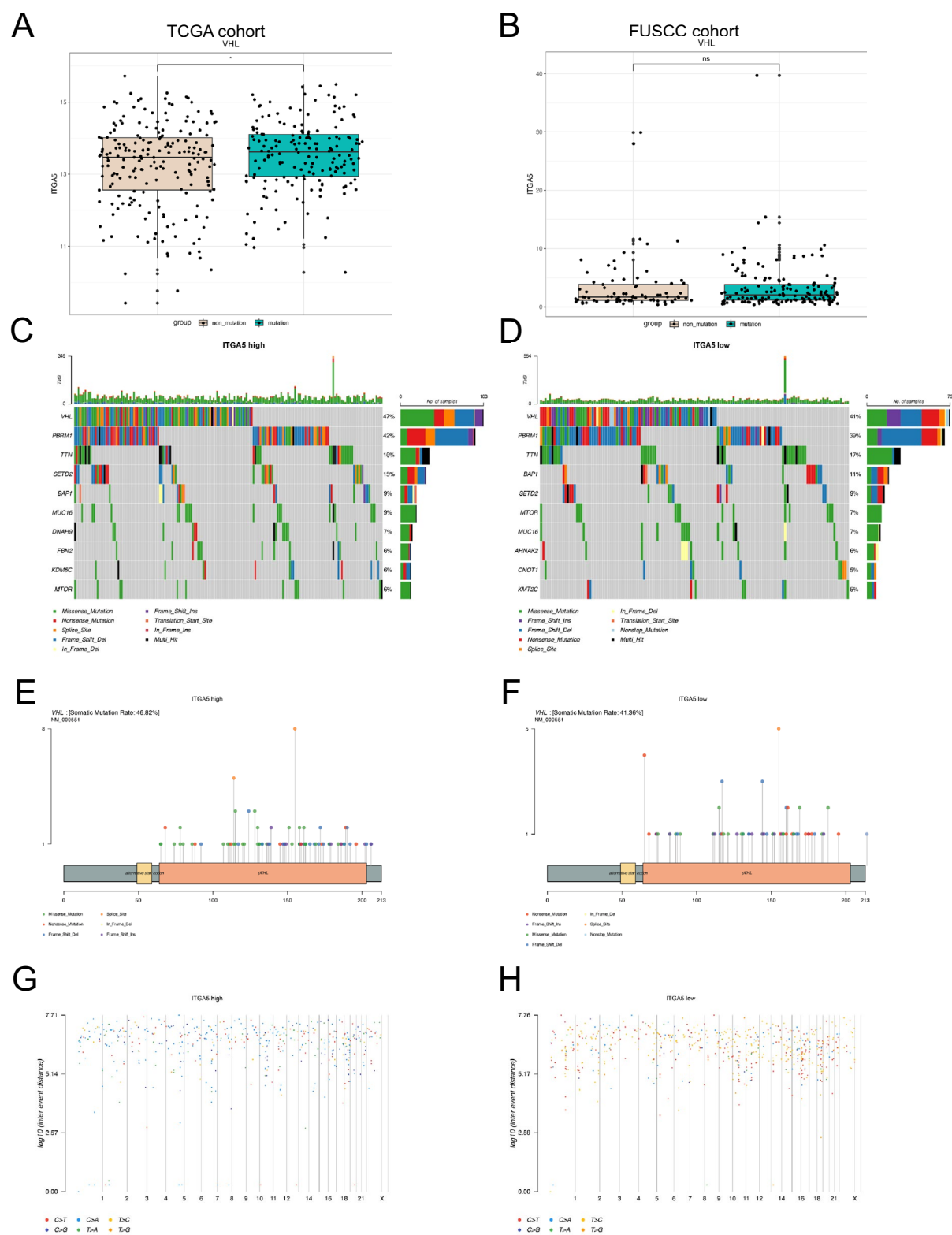


Fig. 3 ITGA5 correlates to typical mutations in ccRCC. **A, B** Correlation between ITGA5 expression and VHL mutation in TCGA cohort and FUSCC cohort. **C, D** Mutation landscape of ITGA5 high/low group. **E, F** VHL mutation sites of ITGA5 high/low group. **G, H** Chromosomal-level base mutation bias

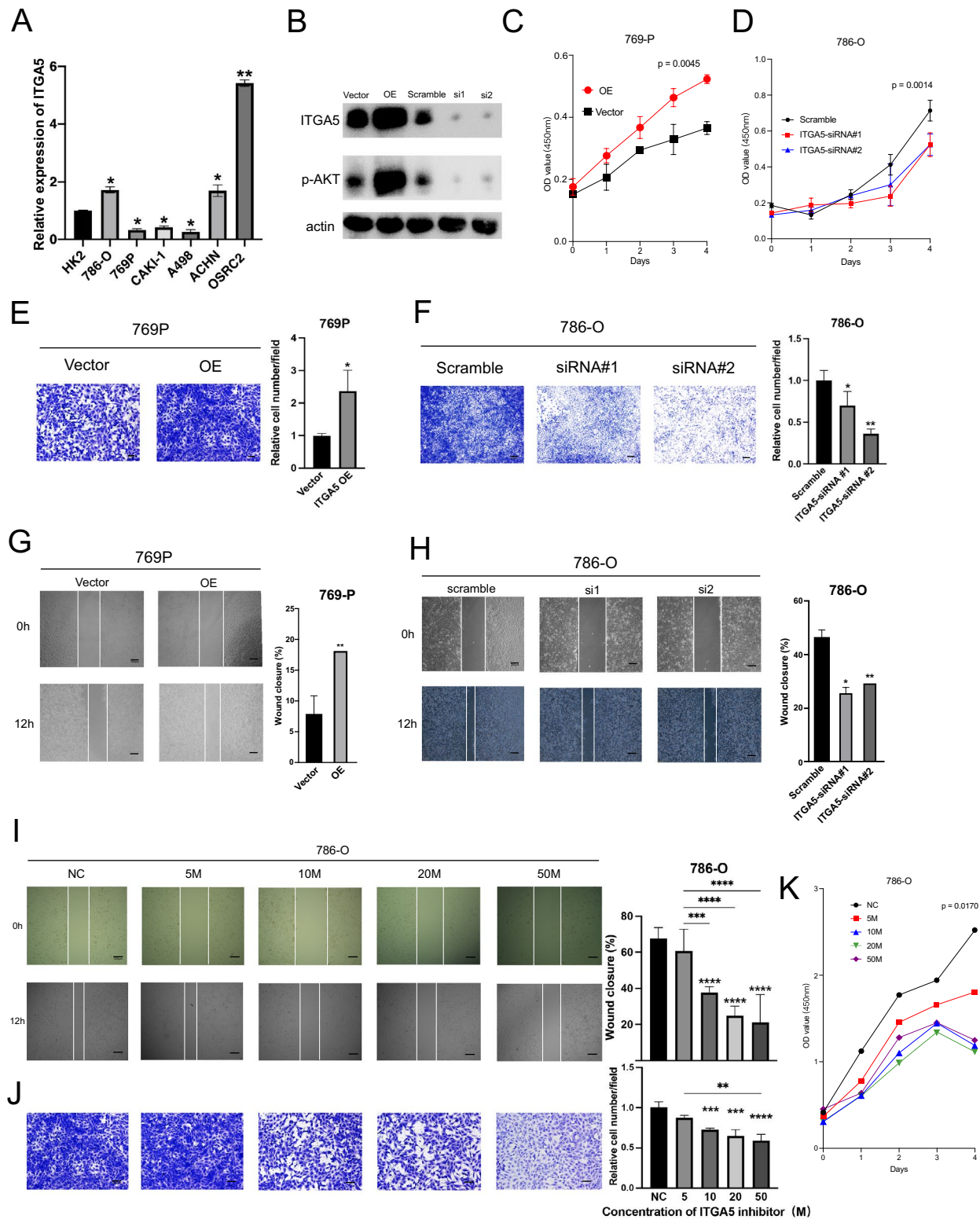


Fig. 4 ITGA5 promotes malignancy and progression of ccRCC. **A** qRT-PCR assay of ITGA5 expression level in types of renal cell carcinoma cell lines. **B** Western blotting assay of ITGA5 expression level in transfected 786-O and 769P cells. **C, D** Cell viability of negative control and transfected cells using cck8 assay. **E, F** Effect of transfection on cell invasion using transwell assay. **G, H** Cell migration ability of processed 786-O and 769P cells using wound healing assay. **I–K** 786-O migration, invasion ability, and cell viability regulated by ITGA5 inhibitors

Molecular function prediction of ITGA5 in ccRCC

To elucidate the mechanisms underlying ITGA5's role in ccRCC, we employed a multifaceted approach, including analysis of the KEGG database, GO, and GSEA. Not surprisingly, analysis of KEGG database through comparison between ITGA5 high and low expressing TCGA cohort was marked by the significant enrichment of PI3K-Akt signaling pathway. Furthermore, the enrichment of focal adhesion and ECM-receptor interaction supported the expected role of ITGA5, an integrin family member, in mediating adhesion of various ECM components as a member of integrin family (Fig. 5A). Activation of the three pathways indicated respectively enhancement of tumor cells in proliferation, invasion/metastasis, and anti-apoptosis ability, suggesting comprehensive potentials of ITGA5 in tumor progression.

Moving beyond the KEGG analysis, molecular function prediction of ITGA5 predicted via GO provided further insights into comprehensive interpretation of ITGA5 influence on ccRCC (Fig. 5B). Cadherin binding was activated significantly; cadherin, as a fundamental signaling mediator in cell–cell contact [39], could be associated with metastasis of tumor. Besides, the enrichment of multiple kinase activities, particularly serine/threonine kinase, highlighted the potential role of ITGA5 in cell viability, given the established role of kinases in ccRCC development. These results indicated a reprogrammed cellular landscape of ITGA5-high tumors.

Complementing these findings, GSEA identified enrichment of multiple pathways in the ITGA5-high population, encompassing proliferation, immune response, angiogenesis, apoptosis, and UV resistance (Fig. 5C). Importantly, the hypoxia hallmark, a common and crucial feature of ccRCC, was activated, coherent to the previously observed correlation between ITGA5 expression and VHL mutation (Fig. 5D). Moreover, enrichment of the G2M, E2F, and epithelial-mesenchymal transition (EMT) hallmarks (Fig. 5D) indicated ITGA5 involvement in ccRCC growth and advancement. Consistent with ITGA5 functions predicted by previous studies [40], angiogenesis pathway was enriched in ITGA5-high group, suggesting its potential as a pro-angiogenic factor. These analyses respectively revealed different functions of ITGA5.

To further investigate the functional network of ITGA5, we constructed PPI network to decipher relevant gene network of ITGA5. GeneMANIA was used to search for proteins having likely interaction with ITGA5, including protein–protein, protein-DNA interactions, pathways, physiological and biochemical reactions, co-expression, co-localization. The top 20 genes were lay out as a circle (Fig. 5E). Another protein–protein interaction network was constructed using differentially expressed

genes in ITGA5 low and high groups (Fig. 5F). Hub genes were calculated by DMNC algorithm in CytoHubba plugin. ITGA5 was recognized as one of the hub genes and showed interaction with TGFB1, HSPG2, LOXL2, COL5A1, ITGBL1, COL6A3, and LTBP1. Both networks identified the significance of ECM components, which supports the close interaction of ITGA5 with ECM.

Finally, to explore the cell-type-specific roles of ITGA5, public single-cell RNA sequencing data revealed predominant expression of ITGA5 in endothelial and macrophage cells (Fig. 5G, H), which aligns with the observed enrichment of the angiogenesis pathway. Further analysis of TCGA RNA-seq data confirmed positive correlations between ITGA5 expression and pro-angiogenic factors like HIF1A, PDGFA, VEGFA, and ANGPT2 (Fig. 5I). These findings collectively highlight the critical role of ITGA5 in ccRCC angiogenesis, suggesting the potential of ITGA5 blockade as a therapeutic strategy in combination with anti-angiogenic drugs.

ITGA5 participates in regulating ccRCC immune TME

Given the prominent distribution of ITGA5 in macrophages and endothelial cells, which could influence the immune landscape of ccRCC [41], we further investigated the role of ITGA5 in shaping ccRCC immune TME. Our previous GSEA analysis identified enrichment of immune response-related pathways, including complement, IL2-STAT5, IFN- γ , and TNF- α signaling (Fig. 6A). These findings prompted us to explore potential links between ITGA5 expression and the immune TME.

Analysis of TCGA RNA-seq data revealed the positive correlation between ITGA5 expression and stromal score via Estimate algorithm, suggesting a likely immunosuppressive TME (Fig. 6B). Then we questioned about the immune cell populations in the TME; CIBERSORT algorithm was utilized to predict abundancy of different cell types (Fig. 6C). ITGA5 expression positively correlated with the abundance of memory resting CD4+T cells, resting NK cells, and macrophages. Conversely, it negatively correlated with follicular helper T cells, regulatory T cells, and most importantly, CD8+T cells. These observations could be attributed to ITGA5's potential role in immune cell migration. Notably, the enrichment of macrophages further corroborated the previous finding of ITGA5's influence on macrophage recruitment. Besides, despite not any statistical significance, a tendency of M2 polarization of macrophages was observed, which could be one of mechanisms by which ITGA5 might modulate the immune TME. Also, we performed correlation analysis between ITGA5 and immune infiltration level for ccRCC; scatter plots were generated with partial Spearman's correlation and statistical significance,

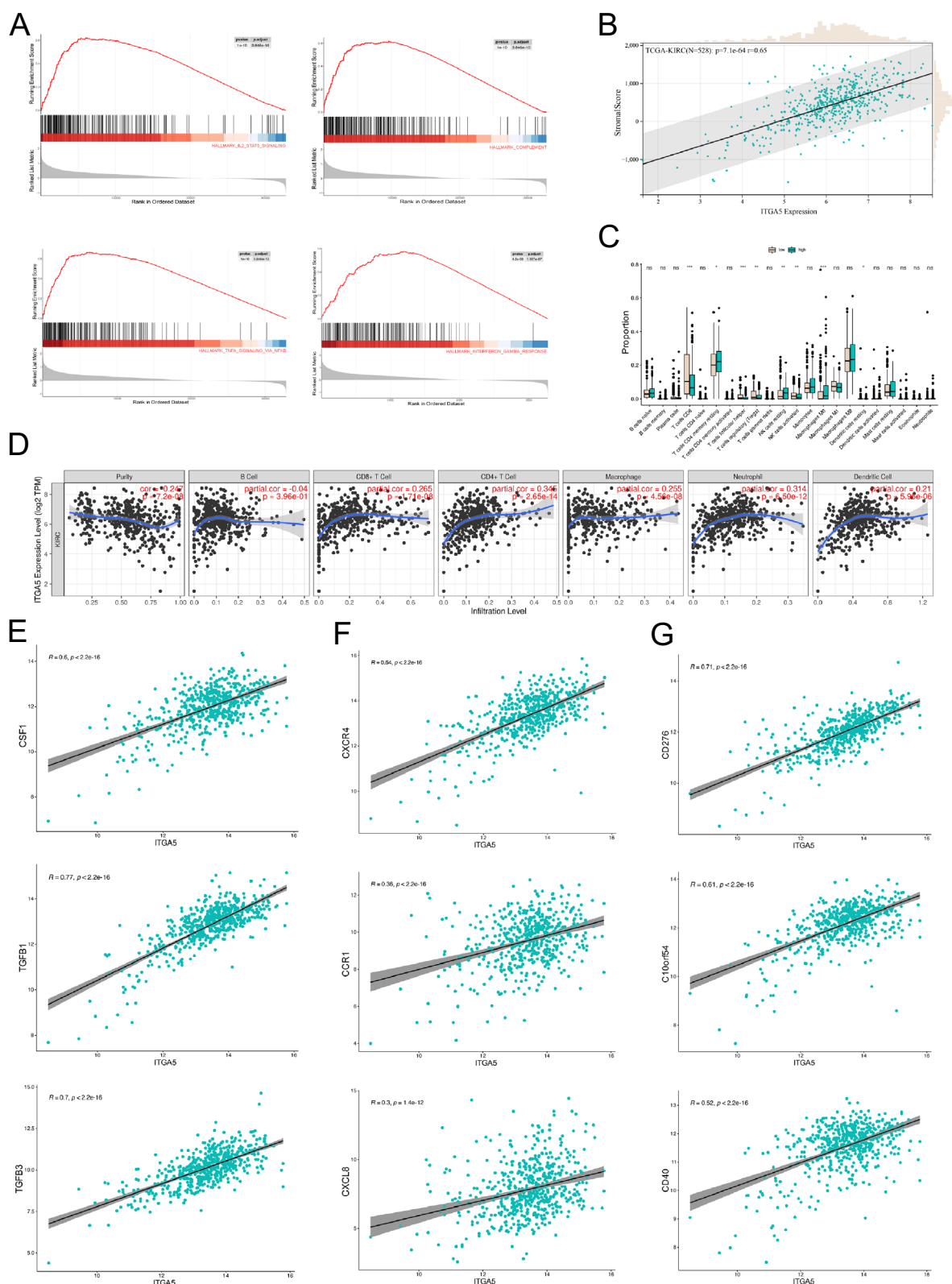


Fig. 6 ITGA5 participates in regulating ccRCC immune TME. **A** Activated pathways relevant to tumor immune response. **B** CIBERSORT estimation of immune cell proportion in ccRCC TME. **C** Correlation between stromal score and ITGA5 expression. **D** Immune infiltration landscape in the TME. **E–G** Expression correlation analysis between ITGA5 and cytokines, chemokines, and immunoregulatory molecules

revealing an ITGA5-related immune infiltration level similar to that predicted previously (Fig. 6D).

To elucidate the mechanisms underlying ITGA5-mediated TME reprogramming, we examined co-expression patterns between ITGA5 and cytokines/chemokines and showed the top-ranked ones (Fig. 6E, F). CSF1, TGFB1, and TGFB3 shared a strong correlation in expression level with ITGA5 (Fig. 6E). CSF1 plays a crucial role in the recruitment, differentiation, and survival of monocytes and macrophages, while TGFB family is well recognized as a powerful driver in angiogenesis and desmoplasia. Comparatively, the correlation between chemokines or its receptor and ITGA5 was weaker; however, the observed positive correlation between ITGA5 and CCR1/CXCL8, both implicated in macrophage recruitment, further supports our previous findings on ITGA5's role in macrophage chemotaxis (Fig. 6F). Lastly, co-expression analysis revealed a positive correlation between ITGA5 and immune regulatory molecules, including immune checkpoint ligands CD276 (B7-H3) and C10orf54 (VISTA) (Fig. 6G), suggesting that T cells in ccRCC TME with high expression of ITGA5 were likely to be exhausted. Generally, we believed that ITGA5 high expressed ccRCC has an immunosuppressive TME.

Exploration of therapeutic target relevant to ITGA5

To explore the potential clinical implications of ITGA5 expression, we further performed drug sensitivity analysis using the R package pRRophetic. We focused on 18 drugs commonly used for non-solid tumors, excluding chemotherapeutic agents due to their limited efficacy in ccRCC under most circumstances. Analysis of predicted IC50 values revealed significant differences in drug sensitivity between ITGA5-high and ITGA5-low groups for 11 drugs (Fig. 7).

High group were predicted to be more responsive to 7 drugs (Fig. 7A–G). Not surprisingly, VEGFR-targeted drugs, referring to axitinib, sunitinib, pazopanib, and AMD.706 (motesanib) were expected to have greater killing capacity on ITGA5-high-expressed ccRCC cells (Fig. 7A–D); axitinib, sunitinib, and pazopanib are already included in the first-line treatment regimens for ccRCC patients. These findings suggest that ITGA5 expression could be a valuable biomarker for guiding treatment decisions. Moreover, a combination strategy of ITGA5 inhibitors with anti-VEGFR drugs might be particularly beneficial for ITGA5-high patients.

Interestingly, the high group exhibited increased predicted sensitivity to poly (ADP-ribose) polymerase (PARP) inhibitors, including AZD.2281 (olaparib) and AG.014699 (rucaparib) (Fig. 7E, F). While TKI and immunotherapy are the mainstays of ccRCC treatment, studies also showed the potential of PARP inhibitors in

treating ccRCC, particularly in PMRB1 and SETD2 deficient patients [42, 43]. Moreover, our previous results showed that there was a tendency of upregulation of ITGA5 expression in SETD2 mutant patients (Figure S1E, S1J), potentially contributing to increased sensitivity to PARP inhibitors in this subgroup. Additionally, temsirolimus, targeting mTOR complex, was also likely to be beneficial in ITGA5 high expressed ccRCC over ITGA5 low ones (Fig. 7G); in the second-line treatment mTOR inhibitors are treatment choices. Moreover, we observed the lowest inhibitory concentration in temsirolimus, which highlighted its likely strong efficacy in treating ITGA5 high populations.

Conversely, the ITGA5-high group also displayed resistance to several agents (Fig. 7H–K). These included lapatinib, BIBW2992 (afatinib), erlotinib, and gefitinib, which are all clinically used anti-EGFR TKI. Further, as ICB therapy was also recommended for ccRCC patients as TKIs, we evaluated response to ICB through TIDE score in ITGA5 high/low groups. Interestingly, despite the co-expression of ITGA5 and multiple immune checkpoints, ITGA5-high group showed poorer sensitivity to ICB (Fig. 7L); this observation, despite the co-expression of ITGA5 and immune checkpoint ligands, could be attributed to reduced infiltration of CD8+ T cells.

Taken together, we could make clinical implications that the combination of anti-angiogenetic drugs and ITGA5 inhibitors might acquire considerable clinical bonus in ITGA5 high expressed ccRCC patients.

Discussion and conclusion

The integrin family are responsible for mediating cell adhesion and intercell signal transmission. This family of adhesion receptors could regulate complex cellular behaviors including survival, proliferation, migration, and various cell fate transitions [44, 45]. Integrin activation often involves the FAK-Src signaling pathway [46]. High expression of specific integrins, including $\alpha\beta3$, $\alpha\beta5$, $\alpha5\beta1$, $\alpha6\beta4$, $\alpha4\beta1$ and $\alpha\beta6$ is correlated with tumor progression [47–52]. Notably, integrin $\alpha\beta3$, $\alpha5\beta1$ and $\alpha\beta6$, are usually expressed at low or undetectable levels in most adult epithelia but can be upregulated in some tumors. As a member of alpha integrin subgroup, ITGA5 was identified by previous studies as an oncologic-promoting factor in multiple cancer types [13, 15, 17, 40, 53]. In this study, we demonstrated the prognostic significance of ITGA5 in ccRCC. With the hub genes selected by lasso regression model, we constructed an XGBoost-generated prognosis model and verified the robust power of this model using ROC curve, calibration, and DCA plot. Consistent with research in other tumor types, ITGA5 emerged as a detrimental biomarker in ccRCC. Besides, we tried to explain the role of ITGA5

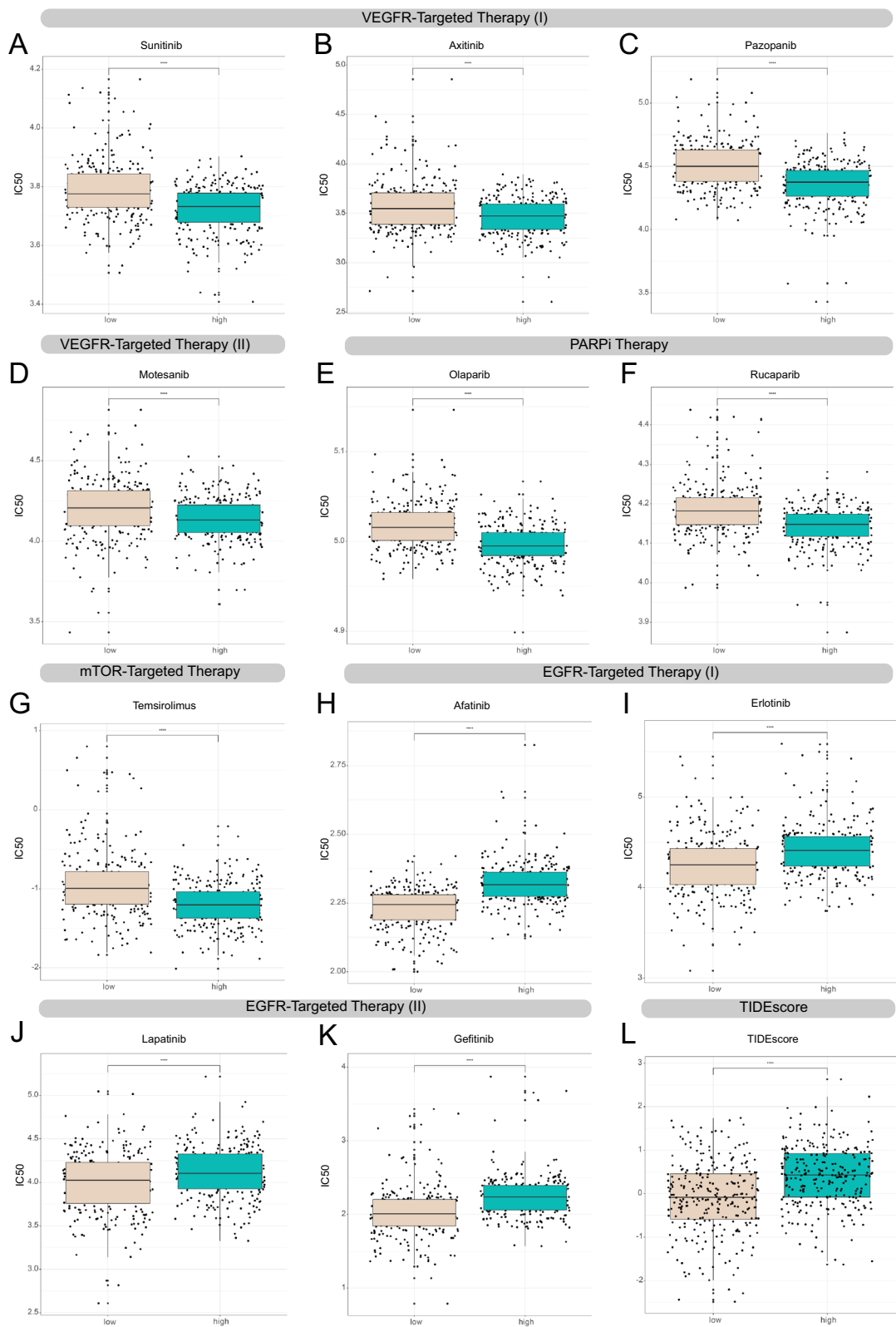


Fig. 7 Exploration of therapeutic target relevant to ITGA5. **A–D** VEGFR-targeted drug sensitivity of ITGA5 differently expressed populations. **E–F** Response to PARP inhibitors. **G** Effect prediction of temsirolimus. **H–K** Predicted outcome of EGFR-targeted therapies. **L** Difference of TIDE score between ITGA5 high/low groups

from the perspective of ccRCC tumorigenesis; we analyzed the correlation between ITGA5 expression level and frequently mutant genes in ccRCC, which implied a potential co-regulatory relationship between ITGA5 and these mutations, especially VHL mutation. Current studies usually linked ITGA5 with tumorigenesis via activation of PI3K pathway or mTORC1 [53, 54]; while our results offered new insights into potential mechanisms underlying ITGA5 interaction with ccRCC pathogenic mutant genes.

This study comprehensively described the potential functions of ITGA5 and activated pathways by ITGA5 in ccRCC. Our findings demonstrated that ITGA5 primarily promotes tumor progression through inducing proliferation, cell migration, angiogenesis, and drug resistance, which aligns with previous observations in other cancer types [14, 40]. We also performed an in-depth analysis of immune cell infiltration in tumors with varying ITGA5 expression levels. Previous studies mostly failed to elaborate detailed information on the infiltration of specific cell types [17, 20]; our results, however, revealed a specific chemokine-like function of ITGA5 in macrophage recruitment. Generally, tumors with high level of ITGA5 expression displayed an immunosuppressive TME. The mechanisms underlying this immunosuppressive environment remain to be elucidated, but two potential explanations include the direct effect of ITGA5 on cell migration and ITGA5-induced desmoplasia [28], given the recognized fact that desmoplasia also promotes immune exclusion [55, 56]. Our results verified the co-expression of ITGA5 and TGF β family, which hints on the potential pro-desmoplastic and immunosuppression-inducing role of ITGA5 in ccRCC.

Integrins have been an attractive therapeutic target and antagonists for integrins are under development. For instance, LM609, an α v β 3 antagonist, which was among the first integrin monoclonal antibodies developed, showed significant anti-angiogenic activity in preclinical models [57]. Its humanized version, named Etaracizumab (MEDI-522), exhibited anti-angiogenic effects and additionally inhibited tumor growth [58]. In a phase I clinical trial for renal cell carcinoma, it showed promising results regarding tumor perfusion with minimal toxicity [59]. Strategies that target β 1 integrins, particularly α 5 β 1, have also shown efficacy in reducing tumor burden, as exemplified by volociximab, which inhibited angiogenesis and tumor growth in a phase I trial [60]. However, to our knowledge, no clinical trials have yet investigated α 5 integrin (ITGA5) monoclonal antibodies. Our findings, combined with previous studies, suggest that targeting ITGA5 holds promise as a therapeutic strategy for ccRCC. We validated the efficacy of a specific ITGA5 inhibitor originally proposed for pancreatic cancer

featured by reduced perfusion, demonstrating its optimal in vitro effects in ccRCC, a cancer type characterized by prominent angiogenesis.

To find out therapeutic implications of ITGA5 on currently available drugs, we further explored the drug sensitivity landscape of tumors with varying ITGA5 expression using the pRRophetic package. Our analysis suggests that the ITGA5-high group might respond favorably to anti-VEGFR TKIs, indicating the potential for combining ITGA5 inhibitors with first-line anti-VEGFR monoclonal antibodies in ccRCC treatment [61]. Besides, this group might exhibit sensitivity to PARP inhibitors. Despite the absence of PARP inhibitors in the recommended treatment regimen for ccRCC patients, further research is warranted to optimize treatment outcomes for specific patient populations, considering the emergence of PARP inhibitors as a powerful new class of anti-cancer drugs. Our results identified ITGA5 as a biomarker of PARP inhibitor application. Conversely, anti-EGFR therapies might be less effective against ITGA5-high tumors. Although anti-EGFR TKIs are not typically used in ccRCC treatment, clinical trials have been carried out to explore their efficacy in combination with first-line drugs for EGFR-expressing tumors. These trials yielded heterogeneous outcomes in renal cell carcinoma [62–64]; our results might partially explain this disparity since ITGA5 could be a potential negative biomarker for this type of TKI.

As ICB therapy has revolutionized cancer treatment by targeting the immune TME, we focus on ITGA5 effect on ICB therapy efficacy to promote precision medication. The European Association of Urology guideline on renal cell carcinoma recommended ICB therapy as the backbone for treatment-naïve metastatic ccRCC, often complemented by a TKI or a second ICI directed against CTLA-4 [5]. While PD-L1 expression in tumors has been extensively studied as a predictor of ICB response, some patients with low or undetectable PD-L1 levels still experience positive responses [65]. The obstruction of development for ICB biomarkers could be explained by the complexity of mediators involved in anti-tumor responses and the heterogeneity of RCC, highlighting the ongoing need for research on ICB response biomarkers. We depicted the immune landscape of ccRCC with different expression level of ITGA5 and identified ITGA5 as a potential predictor for ICB resistance. This could be caused by the migration of specific immune cell type induced by ITGA5; particularly, the infiltration of CD8 $^{+}$ T cell was downregulated in ITGA5 high group. A comprehensive evaluation of ICB response could consider ITGA5 expression alongside other factors.

In conclusion, our findings clarified the adverse outcome induced by elevated ITGA5 expression in ccRCC.

In vitro experiments and bioinformatical analysis identified the comprehensive function of ITGA5 and predicted immune infiltration and medication sensitivity regulation. However, we recognize the inherent limitations of bioinformatical analyses, including potential biases related to data sources and computational predictions. Additionally, further in vivo experiments are necessary to elucidate the underlying mechanisms and confirm the clinical efficacy of ITGA5 inhibition. Moreover, variability in ITGA5 expression across different patient cohorts should be acknowledged, and validation in independent cohorts is essential to broaden its clinical significance. Despite these limitations, we believe that integrins, including ITGA5, remain promising therapeutic targets. By integrating ITGA5 analysis with current treatment strategies, there is potential to develop more personalized and effective therapies for ccRCC patients [66].

Abbreviations

AUC	Area under the curve
CCL	Cancer Cell Line Encyclopedia
ccRCC	Clear cell renal cell carcinoma
ECM	Extracellular matrix
FUSCC	Fudan University Shanghai Cancer Center
GEO	Gene Expression Omnibus
GSEA	Gene set enrichment analysis
GO	Gene Ontology
ICB	Immune checkpoint blockade
KEGG	Kyoto Encyclopedia of Genes and Genomes
TCGA	The Cancer Genome Atlas
TME	Tumor microenvironment
TKI	Tyrosine kinase inhibitors
XGBoost	eXtreme Gradient Boosting

Supplementary Information

The online version contains supplementary material available at <https://doi.org/10.1186/s12935-024-03546-4>.

Additional file1.

Additional file2.

Acknowledgements

We express our sincere gratitude to Professor Jai Prakash from University of Twente, Enschede, Netherlands (j.prakash@utwente.nl) for his guidance in the peptidomimetic aspect of this research. We thank the TCGA, GEO database for providing RNA-seq data and clinical information of ccRCC. We also thank all the investigators, study nurses, patients and their family members who participated in this study.

Author contributions

The work reported in the paper has been performed by the authors, unless clearly specified in the text. XC, XT, ZW, WX, HZ, and DY worked for the conception and design of this research. XC, XT, ZW, SZ, SY, and AA collected and assembled data and analysis part was finished by XC, XT, ZW, YC, YH, PY, YC, KW, and YL. XC, XT, ZW, SZ, SY, and YW performed in vitro experiments. XC, XT, ZW, and HZ prepared the figures and wrote the main manuscript. The manuscript was finally edited and approved by WX, HZ, and DY. XC, HZ, and DY participated in fund acquisition.

Funding

This work is supported FDUOP (Fudan Undergraduate Research Opportunities Program) (22401), Shanghai Undergraduate Training Program on

Innovation and Entrepreneurship (SUTPLE) grant (S202310246246), Beijing Xisike Clinical Oncology Research Foundation (No. Y-HR2020MS-0948), the Shanghai Anti-Cancer Association Eysa Project (No. SACA-CY23A02, SACA-CY23C04), Shanghai Municipal Health Bureau (No.2020CXJQ03).

Data availability

Gene expression and corresponding clinical information of 908 ccRCC samples from 6 cohorts as follow: 535 ccRCC samples from TCGA cohort (<https://www.cancer.gov/about-nci/organization/ccg/research/structural-genomics/tcga>), 232 ccRCC samples from FUSCC cohort (<https://www.nature.com/articles/s41467-022-29577-x#data-availability>), 53 ccRCC samples from GSE53000 cohort, 72 ccRCC samples from GSE53757 cohort, 14 ccRCC samples from GSE145281 cohort, and 2 ccRCC samples from GSE171306 cohort (<https://www.ncbi.nlm.nih.gov/geo/query/acc.cgi>). No datasets were generated or analysed during the current study.

Declarations

Ethics approval and consent to participate

Not applicable.

Competing interests

The authors declare no competing interests.

Author details

¹Department of Urology, Fudan University Shanghai Cancer Center, No. 270 Dong'an Road, Shanghai 200032, People's Republic of China. ²Shanghai Genitourinary Cancer Institute, Shanghai 200032, People's Republic of China. ³Department of Oncology, Fudan University Shanghai Medical College, Shanghai 200032, People's Republic of China. ⁴School of Informatics, Xiamen University, Xiamen 361102, People's Republic of China.

Received: 24 April 2024 Accepted: 24 October 2024

Published: 5 November 2024

References

1. Siegel RL, Giaquinto AN, Jemal A. Cancer statistics, 2024. *CA Cancer J Clin*. 2024;74(1):12–49.
2. Zheng R, et al. Cancer incidence and mortality in China, 2016. *J Natl Cancer Center*. 2022;2(1):1–9.
3. Hegde PS, Chen DS. Top 10 challenges in cancer immunotherapy. *Immunity*. 2020;52(1):17–35.
4. Rooney MS, et al. Molecular and genetic properties of tumors associated with local immune cytolytic activity. *Cell*. 2015;160(1–2):48–61.
5. Ljungberg B, et al. European Association of Urology Guidelines on renal cell carcinoma: the 2022 update. *Eur Urol*. 2022;82(4):399–410.
6. Motzer RJ, et al. Kidney cancer, version 3.2022, NCCN clinical practice guidelines in oncology. *J Natl Compr Canc Netw*. 2022;20(1):71–90.
7. McDermott DF, et al. Clinical activity and molecular correlates of response to atezolizumab alone or in combination with bevacizumab versus sunitinib in renal cell carcinoma. *Nat Med*. 2018;24(6):749–57.
8. Şenbabaoğlu Y, et al. Tumor immune microenvironment characterization in clear cell renal cell carcinoma identifies prognostic and immunotherapeutically relevant messenger RNA signatures. *Genome Biol*. 2016;17(1):231.
9. Desgrosellier JS, Cheresh DA. Integrins in cancer: biological implications and therapeutic opportunities. *Nat Rev Cancer*. 2010;10(1):9–22.
10. Stupack DG, et al. Apoptosis of adherent cells by recruitment of caspase-8 to unligated integrins. *J Cell Biol*. 2001;155(3):459–70.
11. Avraamides CJ, Garmy-Susini B, Varner JA. Integrins in angiogenesis and lymphangiogenesis. *Nat Rev Cancer*. 2008;8(8):604–17.
12. Kennelly TM, et al. Distinct binding interactions of $\alpha(5)\beta(1)$ -integrin and proteoglycans with fibronectin. *Biophys J*. 2019;117(4):688–95.
13. Li XQ, et al. Extracellular vesicle-packaged CDH11 and ITGA5 induce the premetastatic niche for bone colonization of breast cancer cells. *Cancer Res*. 2022;82(8):1560–74.

14. Shi Y, et al. ITGA5 predicts dual-drug resistance to temozolomide and bevacizumab in glioma. *Front Oncol*. 2021;11: 769592.
15. Li XF, et al. Macrophages promote anti-androgen resistance in prostate cancer bone disease. *J Exp Med*. 2023. <https://doi.org/10.1084/jem.20221007>.
16. Zhang C, et al. Coupling of integrin $\alpha 5$ to annexin A2 by flow drives endothelial activation. *Circ Res*. 2020;127(8):1074–90.
17. Zhu H, et al. ITGA5 is a prognostic biomarker and correlated with immune infiltration in gastrointestinal tumors. *BMC Cancer*. 2021;21(1):269.
18. Shaim H, et al. Targeting the αv integrin/TGF- β axis improves natural killer cell function against glioblastoma stem cells. *J Clin Invest*. 2021. <https://doi.org/10.1172/JCI142116>.
19. Lu L, et al. Targeting integrin $\alpha 5$ in fibroblasts potentiates colorectal cancer response to PD-L1 blockade by affecting extracellular-matrix deposition. *J Immunother Cancer*. 2023. <https://doi.org/10.1136/jitc-2023-007447>.
20. Li S, et al. ITGA5 is a novel oncogenic biomarker and correlates with tumor immune microenvironment in gliomas. *Front Oncol*. 2022;12: 844144.
21. Qu Y, et al. A proteogenomic analysis of clear cell renal cell carcinoma in a Chinese population. *Nat Commun*. 2022;13(1):2052.
22. Ritchie ME, et al. Limma powers differential expression analyses for RNA-sequencing and microarray studies. *Nucleic Acids Res*. 2015;43(7): e47.
23. Tsherniak A, et al. Defining a cancer dependency map. *Cell*. 2017;170(3):564–576.e16.
24. Meyers RM, et al. Computational correction of copy number effect improves specificity of CRISPR-Cas9 essentiality screens in cancer cells. *Nat Genet*. 2017;49(12):1779–84.
25. Chen T, Guestrin C. Xgboost: a scalable tree boosting system. In *Proceedings of the 22nd acm sigkdd international conference on knowledge discovery and data mining*. 2016.
26. Qu YY, et al. Inactivation of the AMPK-GATA3-ECHS1 pathway induces fatty acid synthesis that promotes clear cell renal cell carcinoma growth. *Cancer Res*. 2020;80(2):319–33.
27. Xu W, et al. Tumor-associated macrophage-derived chemokine CCL5 facilitates the progression and immunosuppressive tumor microenvironment of clear cell renal cell carcinoma. *Int J Biol Sci*. 2022;18(13):4884–900.
28. Kuninty PR, et al. ITGA5 inhibition in pancreatic stellate cells attenuates desmoplasia and potentiates efficacy of chemotherapy in pancreatic cancer. *Sci Adv*. 2019;5(9):eaax2770.
29. Subramanian A, et al. Gene set enrichment analysis: a knowledge-based approach for interpreting genome-wide expression profiles. *Proc Natl Acad Sci USA*. 2005;102(43):15545–50.
30. Franz M, et al. GeneMANIA update 2018. *Nucleic Acids Res*. 2018;46(W1):W60–w64.
31. Franceschini A, et al. STRING v91: protein-protein interaction networks, with increased coverage and integration. *Nucleic Acids Res*. 2013;41:D808–15.
32. Yoshihara K, et al. Inferring tumour purity and stromal and immune cell admixture from expression data. *Nat Commun*. 2013;4:2612.
33. Newman AM, et al. Robust enumeration of cell subsets from tissue expression profiles. *Nat Methods*. 2015;12(5):453–7.
34. Gleeleher P, Cox N, Huang RS. pRRophetic: an R package for prediction of clinical chemotherapeutic response from tumor gene expression levels. *PLoS One*. 2014;9(9): e107468.
35. Yang W, et al. Genomics of drug sensitivity in cancer (GDSC): a resource for therapeutic biomarker discovery in cancer cells. *Nucleic Acids Res*. 2013;41:D955–61.
36. Jiang P, et al. Signatures of T cell dysfunction and exclusion predict cancer immunotherapy response. *Nat Med*. 2018;24(10):1550–8.
37. Jonasch E, Walker CL, Rathmell WK. Clear cell renal cell carcinoma ontogeny and mechanisms of lethality. *Nat Rev Nephrol*. 2021;17(4):245–61.
38. Hu J, et al. Tumor heterogeneity in VHL drives metastasis in clear cell renal cell carcinoma. *Signal Transduct Target Ther*. 2023;8(1):155.
39. Maître JL, Heisenberg CP. Three functions of cadherins in cell adhesion. *Curr Biol*. 2013;23(14):R626–33.
40. Xu X, et al. ITGA5 promotes tumor angiogenesis in cervical cancer. *Cancer Med*. 2023;12(10):11983–99.
41. Baradaran A, et al. The cross-talk between tumor-associated macrophages and tumor endothelium: recent advances in macrophage-based cancer immunotherapy. *Biomed Pharmacother*. 2022;146: 112588.
42. Zhou X, et al. SETD2 deficiency confers sensitivity to dual inhibition of DNA methylation and PARP in kidney cancer. *Cancer Res*. 2023;83(22):3813–26.
43. Chabanon RM, et al. PBRM1 deficiency confers synthetic lethality to DNA repair inhibitors in cancer. *Cancer Res*. 2021;81(11):2888–902.
44. Giancotti FG, Ruoslahti E. Integrin signaling. *Science*. 1999;285(5430):1028–32.
45. Hynes RO. Integrins: versatility, modulation, and signaling in cell adhesion. *Cell*. 1992;69(1):11–25.
46. Mitra SK, Schlaepfer DD. Integrin-regulated FAK-Src signaling in normal and cancer cells. *Curr Opin Cell Biol*. 2006;18(5):516–23.
47. Bates RC, et al. Transcriptional activation of integrin $\beta 6$ during the epithelial-mesenchymal transition defines a novel prognostic indicator of aggressive colon carcinoma. *J Clin Invest*. 2005;115(2):339–47.
48. Slack-Davis JK, et al. Vascular cell adhesion molecule-1 is a regulator of ovarian cancer peritoneal metastasis. *Cancer Res*. 2009;69(4):1469–76.
49. Diaz LK, et al. $\beta 4$ integrin subunit gene expression correlates with tumor size and nuclear grade in early breast cancer. *Mod Pathol*. 2005;18(9):1165–75.
50. Bello L, et al. $\alpha (v)\beta 3$ and $\alpha (v)\beta 5$ integrin expression in glioma periphery. *Neurosurgery*. 2001;49(2):380–9 (**Discussion 390**).
51. Adachi M, et al. Significance of integrin $\alpha 5$ gene expression as a prognostic factor in node-negative non-small cell lung cancer. *Clin Cancer Res*. 2000;6(1):96–101.
52. McCabe NP, et al. Prostate cancer specific integrin $\alpha v\beta 3$ modulates bone metastatic growth and tissue remodeling. *Oncogene*. 2007;26(42):6238–43.
53. Yan T, Ye XX. MicroRNA-328-3p inhibits the tumorigenesis of bladder cancer through targeting ITGA5 and inactivating PI3K/AKT pathway. *Eur Rev Med Pharmacol Sci*. 2019;23(12):5139–48.
54. Li D, et al. Elevated ITGA5 facilitates hyperactivated mTORC1-mediated progression of laryngeal squamous cell carcinoma via upregulation of EFNB2. *Theranostics*. 2022;12(17):7431–49.
55. Chen Y, et al. Oncogenic collagen I homotrimers from cancer cells bind to $\alpha 3\beta 1$ integrin and impact tumor microbiome and immunity to promote pancreatic cancer. *Cancer Cell*. 2022;40(8):818–834.e9.
56. Chen Y, et al. Type I collagen deletion in α SMA(+) myofibroblasts augments immune suppression and accelerates progression of pancreatic cancer. *Cancer Cell*. 2021;39(4):548–565.e6.
57. Brooks PC, et al. Antiintegrin $\alpha v\beta 3$ blocks human breast cancer growth and angiogenesis in human skin. *J Clin Invest*. 1995;96(4):1815–22.
58. Mulgrew K, et al. Direct targeting of $\alpha v\beta 3$ integrin on tumor cells with a monoclonal antibody. *Abegrin Mol Cancer Ther*. 2006;5(12):3122–9.
59. McNeel DG, et al. Phase I trial of a monoclonal antibody specific for $\alpha v\beta 3$ integrin (MED-522) in patients with advanced malignancies, including an assessment of effect on tumor perfusion. *Clin Cancer Res*. 2005;11(21):7851–60.
60. Ricart AD, et al. Volociximab, a chimeric monoclonal antibody that specifically binds $\alpha 5\beta 1$ integrin: a phase I, pharmacokinetic, and biological correlative study. *Clin Cancer Res*. 2008;14(23):7924–9.
61. Wang J, Li K. Antiangiogenic therapy: how far is it to upgrade? *Holist Integ Oncol*. 2024;3(1),14. <https://doi.org/10.1007/s44178-024-00081-0>.
62. Ravaud A, et al. Lapatinib versus hormone therapy in patients with advanced renal cell carcinoma: a randomized phase III clinical trial. *J Clin Oncol*. 2008;26(14):2285–91.
63. Hainsworth JD, et al. Treatment of metastatic renal cell carcinoma with a combination of bevacizumab and erlotinib. *J Clin Oncol*. 2005;23(31):7889–96.
64. Dawson NA, et al. A phase II trial of gefitinib (Iressa, ZD1839) in stage IV and recurrent renal cell carcinoma. *Clin Cancer Res*. 2004;10(23):7812–9.
65. Patel SP, Kurzrock R. PD-L1 expression as a predictive biomarker in cancer immunotherapy. *Mol Cancer Ther*. 2015;14(4):847–56.
66. Tang Y, et al. Next-generation sequencing-guided personalized therapy in renal cell carcinoma. *Holist Integ Oncol*. 2024;3(1):4. <https://doi.org/10.1007/s44178-024-00072-1>.

Publisher's Note

Springer Nature remains neutral with regard to jurisdictional claims in published maps and institutional affiliations.